

Power and Bandwidth of Spontaneous Parametric Emission*

R. L. BYER AND S. E. HARRIS

Department of Electrical Engineering, Stanford University, Stanford, California

(Received 20 November 1967)

Theoretical and experimental results concerned with the spectral and angular distribution of spontaneous parametric emission are reported. Such emission results when light from a pumping laser is incident on a nonlinear crystal, and does not require that the parametric gain exceed the single-pass crystal loss. The emission is somewhat like spontaneous Raman or Brillouin scattering, but differs in two major respects. First, in a lossless crystal, the bandwidth of the emission is controlled by the crystal length and accepted angular aperture as opposed to a loss mechanism in the Raman or Brillouin case. Second, by changing the crystal temperature or orientation, the spontaneous emission may be tuned over several thousand angstroms. The reported experiments employed a 4880 Å laser as a pump and a 1-cm crystal of LiNbO₃ as the nonlinear material. The application of parametric spontaneous emission to the measurement of crystal nonlinearities is considered, and the advantages of this method over second-harmonic generation are discussed.

I. INTRODUCTION

IF light from a pumping laser is incident on a nonlinear crystal whose temperature and angular orientation are such that the momentum matching condition $\mathbf{k}_s + \mathbf{k}_i = \mathbf{k}_p$ is satisfied at three frequencies and such that $\nu_s + \nu_i = \nu_p$, then for a sufficiently strong pumping field, parametric amplification or oscillation may occur.^{1,2} However, even for weaker pumping strengths such that the single-pass parametric gain does not exceed the single-pass absorption loss, there still exists a quantum-mechanical probability that a driving pump photon will split into a signal and idler photon. Such spontaneous parametric emission has been predicted and studied by Louisell *et al.*³ and others,⁴⁻⁷ and has recently been observed at optical frequencies on a pulsed basis by Khokhlov *et al.*⁸ and by Magde and Mahr,⁹ and on a cw basis by Harris *et al.*¹⁰ and by Smith *et al.*¹¹

The properties of spontaneous parametric emission are very much like those of spontaneous Brillouin and Raman scattering. The principal differences are first,

* The research reported in this paper was sponsored by but does not necessarily constitute the opinion of the U. S. Air Force Cambridge Research Laboratories, Office of Aerospace Research, under Contract No. F19628-67-C-0038.

¹ C. C. Wang and C. W. Racette, *Appl. Phys. Letters* **8**, 169 (1965).

² J. A. Giordmaine and Robert C. Miller, *Phys. Rev. Letters* **14**, 973 (1965).

³ W. H. Louisell, A. Yariv, and A. E. Siegman, *Phys. Rev.* **124**, 1645 (1961).

⁴ J. P. Gordon, W. H. Louisell, and L. R. Walker, *Phys. Rev.* **129**, 481 (1963).

⁵ H. Heffner, *Proc. IRE* **50**, 1604 (1962).

⁶ W. G. Wagner and R. W. Hellwarth, *Phys. Rev.* **133**, A915 (1964).

⁷ B. R. Mollow and R. J. Glauber, *Phys. Rev.* **160**, 1076 (1967); **160**, 1097 (1967); D. N. Klyshko, *Zh. Eksperim. i Teor. Fiz. Pisma v Redaktsiyu* **6**, 490 (1967) [English transl.: *Soviet Phys.—JETP Letters* **6**, 23 (1967)].

⁸ R. V. Khokhlov, *Zh. Eksperim. i Teor. Fiz. Pisma v Redaktsiyu* **6**, 575 (1967) [English transl.: *Soviet Phys.—JETP Letters* **6**, 85 (1967)].

⁹ D. Magde and H. Mahr, *Phys. Rev. Letters* **18**, 905 (1967).

¹⁰ S. E. Harris, M. K. Oshman, and R. L. Byer, *Phys. Rev. Letters* **18**, 732 (1967).

¹¹ R. G. Smith, J. G. Skinner, W. Nilsen, and J. E. Geusic, in *Solid State Device Research Conference*, Santa Barbara, California, 1967 (to be published).

that in a lossless medium the bandwidth of the spontaneous parametric emission is controlled by the length of the nonlinear crystal as opposed to the loss-mechanism-controlled bandwidth in the Raman and Brillouin case; and second, by controlling crystal orientation and temperature, parametric spontaneous emission may be tuned for several thousand angstroms.

In this paper we compare theoretical and experimental results based on an argon pumping laser at 4880 Å and a nonlinear crystal of LiNbO₃. The pump is assumed to be a perfectly collimated plane wave incident normally to the crystal face and at 90° to the optic axis of the crystal. The power and spectral distribution of the spontaneous emission are examined as a function of the accepted angular aperture at the output of the crystal.

The application of spontaneous emission to measurement of crystal nonlinearities is also considered.

II. ANALYSIS

In their analysis of noise in parametric processes, Louisell, Yariv, and Siegman³ adopted the simple model of two lossless resonant circuits coupled by a time-varying reactance. By quantizing the electromagnetic

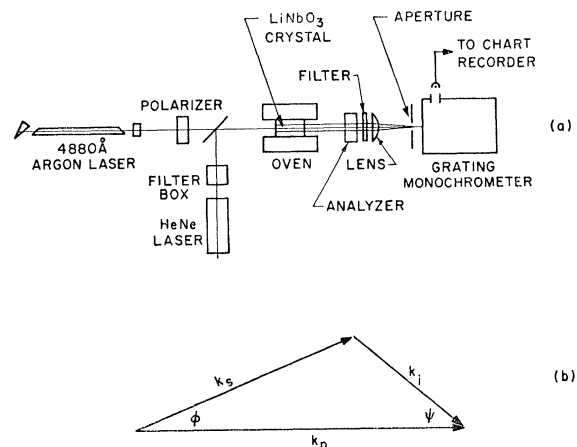


FIG. 1. (a) Schematic of the apparatus. (b) k -vector matching.

fields of the signal and idler modes, they showed that the quantum noise, or in our terms spontaneous emission in the signal channel, would be correctly accounted for by assuming that an extra photon was present at the input of the idler circuit. This result was generalized by Wagner and Hellwarth⁶ to the loss multimode case where one additional photon was to be added for each idler mode coupled to the given signal mode.

In the optical parametric interaction of the present paper, the time-varying reactance of Louisell *et al.*³ is replaced by the nonlinear polarizability of the medium which causes the mixing of the pump, signal, and idler fields. The plan of the present calculation is to assume a plane collimated pump wave, and to allow it to mix with an effective input idler flux which is obtained by allowing one idler photon to be present in each black-body mode of a quantizing volume. The result is a generated signal polarization which attempts to radiate at all signal frequencies and in all directions. Its ability to radiate effectively is determined by the degree of velocity synchronism with the free signal wave at the given frequency and in the given direction.

Consider the experiment shown in Fig. 1(a). The pump beam propagates along the length of the LiNbO₃ crystal and is polarized along its optic axis, such that it is an extraordinary wave. The signal and idler waves are assumed to be ordinary waves and make angles φ and ψ , respectively, with the pump wave. To obtain the effective driving idler power per area we assume a quantizing volume V and assume one idler photon for each mode in the quantizing volume. Multiplying the energy per volume times idler velocity in the medium times the number of modes per interval of \mathbf{k} space, we obtain a differential driving power per area of crystal

$$d\left(\frac{P_i}{A}\right) = \frac{\hbar\nu_i c}{(2\pi)^3 n_i} dk_{ix} dk_{iy} dk_{iz}, \quad (1)$$

where \hbar is Planck's constant, ν_i is the idler frequency in circular units, c is the velocity of light in free space, and n_i is the idler refractive index. By assuming ψ sufficiently small that an increment of solid angle is $2\pi\psi d\psi$ and noting that

$$k_i^2 dk_i = (\nu_i^2/c^3) n_i^3 d\nu_i,$$

Eq. (1) may be rewritten

$$d\left(\frac{P_i}{A}\right) = \frac{\hbar\nu_i^3 n_i^2}{(2\pi)^2 c^2} \psi d\psi d\nu_i. \quad (2)$$

The plane pumping wave is now allowed to mix with all possible idler waves. A pump of wave vector \mathbf{k}_p mixing with an idler wave of wave vector \mathbf{k}_i generates a signal polarization with wave vector $\mathbf{k}_p - \mathbf{k}_i$ and frequency $\nu_p - \nu_i$. The extent to which this polarization wave may effectively radiate is determined by the synchronism between itself and the free signal wave in the given direction. The generated power in any angular

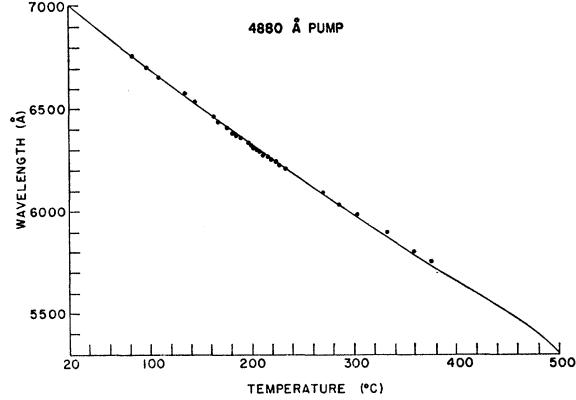


Fig. 2. Signal wavelength versus crystal temperature.

range of signal wave vectors $d\varphi$ and signal frequencies $d\nu_s$ results from the mixing with all idler modes over a corresponding range $d\psi$ with the appropriate frequencies. The incremental radiated power at the signal wavelength is then

$$dP_s = \left(\frac{2\nu_s^2 d_{15}^2}{\epsilon_0^3 c^3 n_s n_i n_p} \right) \frac{P_p}{A} d\left(\frac{P_i}{A}\right) A f(\nu_s, \varphi), \quad (3)$$

where the first collection of constants is the parametric coupling constant. In particular, d_{15} is the crystal nonlinearity such that the generated signal polarization is $2d_{15}E_i(\nu_i)E_p(\nu_p)$, ϵ_0 is the permittivity of free space, n_s , n_i , and n_p are the refractive indices of the signal, idler, and pump, respectively, L is the length of the nonlinear crystal, P_p is the total power of the pumping laser, and A is the crystal area. The factor $f(\varphi, \nu_s)$ is the synchronism reduction factor and is given by

$$f(\nu_s, \varphi) = \frac{\sin^2(|\Delta k| \frac{1}{2} L)}{(|\Delta k| \frac{1}{2} L)^2}, \quad (4)$$

where $|\Delta k|$ is the length of the wave-vector mismatch taken in the pump direction.¹²

For small angles, we have from Fig. 1(b) $\psi d\psi = |k_s/k_i|^2 \varphi d\varphi$. Also, since $\nu_s + \nu_i = \nu_p$, then $d\nu_s = -d\nu_i$. From Eqs. (2) and (3), we then obtain

$$dP_s = \beta L^2 P_p f(\nu_s, \varphi) \varphi d\varphi d\nu_s, \quad (5)$$

where the constant β is given by

$$\beta = \frac{2\nu_s^4 \nu_i d_{15}^2 \hbar n_s}{(2\pi)^2 \epsilon_0^3 c^5 n_i n_p}. \quad (6)$$

To obtain the total radiated power over all frequencies, in a given accepted angle θ , we integrate Eq. (5) and obtain

$$P_s = \beta L^2 P_p \int_{-\infty}^{\infty} \int_0^{\theta} f(\varphi, \nu_s) \varphi d\varphi d\nu_s. \quad (7)$$

¹² D. A. Kleinman, Phys. Rev. **128**, 1761 (1962).

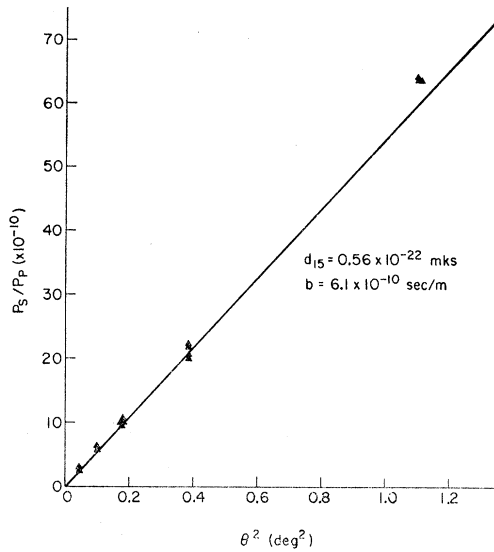


FIG. 3. Total spontaneously emitted power versus θ^2 showing theoretical and experimental results.

We next evaluate the synchronism reduction factor $f(\varphi, \nu_s)$. From Fig. 1(b) we obtain

$$\Delta k = k_p - k_i \cos \psi - k_s \cos \varphi, \quad (8)$$

which for small angles becomes

$$\Delta k = k_p - k_s - k_i + (k_s k_p / k_i)^{1/2} \varphi^2. \quad (9)$$

To account for the dispersion of the refractive indices we assume that at some temperature T_0 , the collinear phase-matching condition $k_{p0} = k_{s0} + k_{i0}$ is satisfied with signal and idler at frequencies ν_{s0} and ν_{i0} . Expanding about these central frequencies we have

$$\begin{aligned} k_s &= k_{s0} + (\partial k_s / \partial \nu_s) d\nu_s, \\ k_i &= k_{i0} - (\partial k_i / \partial \nu_i) d\nu_s, \end{aligned} \quad (10)$$

where we have used $d\nu_i = -d\nu_s$. Substituting Eq. (10) into Eq. (9) and dropping second-order terms we obtain

$$\Delta k = -bd\nu_s + g\varphi^2, \quad (11)$$

where the frequency and angular dispersive constants b and g are given by

$$\begin{aligned} b &= \partial k_s / \partial \nu_s - \partial k_i / \partial \nu_i, \\ g &= k_s k_p / 2k_i. \end{aligned} \quad (12)$$

We note that as a result of normal dispersion $\partial k_s / \partial \nu_s > \partial k_i / \partial \nu_i$, and therefore the angular-frequency behavior is such that higher frequencies are obtained farther off angle.

Combining Eqs. (4), (7), and (12), we obtain

$$P_s = \beta L^2 P_p \int_{-\infty}^{\infty} \int_0^{\theta} \text{sinc}^2[\frac{1}{2}(b\nu_s - g\varphi^2)L] \varphi d\varphi d\nu_s, \quad (13)$$

where $\text{sinc}^2 x \equiv \text{sinc}^2 x / x^2$.

To obtain the total power radiated into an acceptance

angle θ we integrate Eq. (13) which yields

$$P_s = (\beta L P_p / b) \pi \theta^2. \quad (14)$$

The total spontaneously emitted signal power thus varies linearly with accepted solid angle, $\pi \theta^2$, pump power, and crystal length. Noting Eq. (6), it is seen to vary as the fourth power of signal frequency and the first power of idler frequency.

III. DISCUSSION OF RESULTS AND COMPARISON WITH EXPERIMENT

In comparing the predictions of the above analysis with experimental results, we will make use of the numerical approximation to the refractive indices of LiNbO₃ obtained by Hobden and Warner.¹³ As a pumping laser we used a cw argon ion laser, operating at 4880 Å at about the $\frac{1}{2}$ -watt level. The laser operated in the fundamental transverse mode and was collimated to have a beam radius of 0.6 mm. The LiNbO₃ crystal was 1.1 cm long and was mounted in an oven capable of controlling its temperature from room temperature to about 350°C. Temperature calibration was accurate to about 1°C and the temperature was uniform across the length of the crystal to about 0.3°C. As shown in Fig. 1(a), the accepted angular aperture was determined by a stop of variable aperture placed in the focal plane of a lens following the crystal. The accepted angle θ , taken within the nonlinear crystal, is related to the radius r of the stop by

$$\theta = r / n_s f, \quad (15)$$

where f is the focal length of the lens. Spectral measurements were made using a Perkin-Elmer grating spectrometer having a resolution of about 2 Å.

We start by comparing the tuning curve based on the data of Hobden and Warner¹³ with that obtained experimentally. The theoretical curve shown by the solid line in Fig. 2 was obtained by substituting the Hobden-Warner equations for index of refraction into the condition $k_s + k_i = k_p$ and solving numerically for ν_s . Of the different LiNbO₃ crystals which we examined, the experimental points shown in Fig. 2 represent that crystal which showed the best agreement with the Hobden-Warner data and which was thus selected for the remainder of the experiment. Experimental points from other crystals showed the same slope as that of Fig. 2, but their tuning curves were displaced by as much as 30°C from the curve shown. In order to make balance power measurements against a He-Ne laser, the data points in the remainder of the paper were taken at $T = 198^\circ\text{C}$, corresponding to a signal wavelength of 6328 Å.

Next consider the total radiated signal power as a function of accepted solid angle $\pi \theta^2$, without regard to its spectral distribution. From Eqs. (6) and (14) we see that the ratio of spontaneous power to pump power depends upon the nonlinearity squared and inversely

¹³ M. V. Hobden and J. Warner, Phys. Letters **22**, 243 (1966).

upon the constant b . A comparison of the theoretical and experimental results is shown in Fig. 3 where b and d_{15} for the theoretical curve were taken from experimental measurement and Boyd,¹⁴ respectively.¹⁵ The signal power was measured by making a balance measurement against a reference He-Ne laser using calibrated neutral density filters to attenuate the He-Ne beam. The power ratio of the unattenuated He-Ne beam to the 4880 Å pump beam was made with an Eppley thermopile.

We next consider the bandwidth of the spontaneously emitted light as a function of the accepted solid angle $\pi\theta^2$. At a given temperature, dispersion is such that $|k_s| + |k_i|$ increases as the signal frequency moves farther from degenerate. As noted earlier, higher signal frequencies are therefore expected as φ is increased. The theoretical curves of Fig. 4 show signal power as a function of signal frequency for different accepted angles, θ , and were obtained by numerically integrating Eq. (13) between 0 and θ and plotting the resulting $P_s(\nu_s)$. It is noted that $\nu_s=0$ on these curves is the 6328 Å, i.e., the frequency of essentially collinear emission. We note that for the larger accepted solid angles, the spectral distribution of the emitted signal radiation becomes flat topped, and as expected, is skewed toward higher frequencies. As the aperture is closed down the bandwidth is at first reduced, but for small apertures approaches a limiting bandwidth. This limiting bandwidth results since even a collinear parametric interaction may emit over a signal frequency range corresponding to the condition $\Delta kL \cong 2\pi$. In our notation this minimum bandwidth is in cps approximately $1/bL$ and at 6328 Å for our 1.1-cm crystal is about 4 cm^{-1} .

Experimental results are shown on part (c) of Fig. 4, and have been scaled such that the peak of the experimental curve coincides with the peak of the theoretical curve. The total half-power bandwidth and peak intensity as obtained from Fig. 4 are also plotted in Fig. 5 as a function of the accepted angle. We believe that the discrepancy between the theoretical and experimental results is probably due to a difference between the constant b as determined from Hobden and Warner¹³ and the actual b of our crystal. Refractive index inhomogeneities which have been recently reported by Midwinter¹⁶ may also play a part in the difference in minimum bandwidth of the theoretical and experimental curves.

IV. APPLICATION TO MEASUREMENT OF CRYSTAL NONLINEARITIES

The application of spontaneous parametric emission to the measurement of crystal nonlinearities offers a

¹⁴ G. D. Boyd and A. Ashkin, Phys. Rev. **146**, 187 (1966); see p. 191.

¹⁵ We take $d_{15}(\text{LiNbO}_3) = 11 d_{14}(\text{KDP})$ (from Ref. 14) with $d_{14}(\text{KDP})$ as measured by Bjorkholm and Siegman [Phys. Rev. **154**, 857 (1967)]. Thus, in mks units we have $d_{15} = 0.56 \times 10^{-22}$.

¹⁶ J. E. Midwinter, Appl. Phys. Letters **11**, 128 (1967).

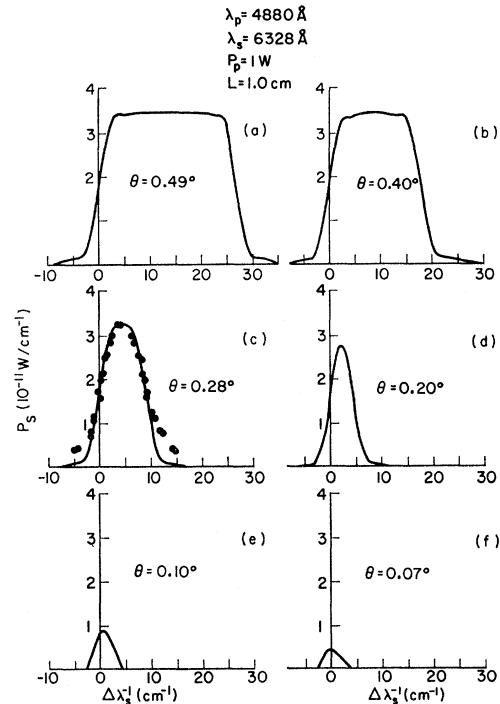


FIG. 4. Spectral distribution of spontaneous power at different acceptance angles. Part (c) shows experimental points normalized to peak of the theoretical curve.

number of potential advantages over the use of second-harmonic generation. First, since the spontaneously emitted power is proportional to the incident power, only a ratio of powers need be measured to determine the nonlinearity. This avoids the difficult task of measuring the absolute powers of pump and second-harmonic signals. Second, as seen from Eq. (14), the magnitude of the spontaneously emitted power is independent of the area of the pumping beam. Furthermore, in the case of multimode pumping lasers, only the average power of the laser is of significance, and the result is not affected by relative mode phases and the

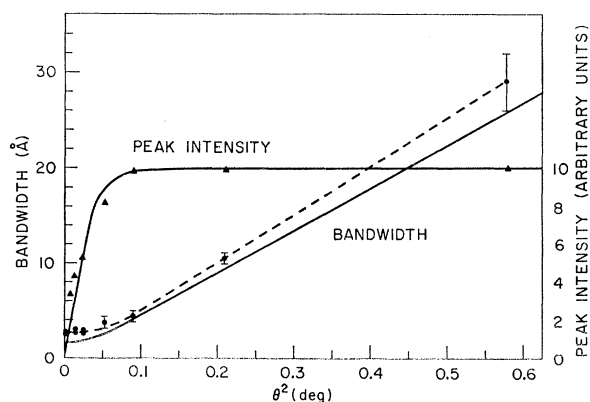


FIG. 5. Peak intensity and bandwidth versus acceptance angle. The solid line is theoretical and the dotted line is experimental.

possibility of self-phase locking.¹⁴ Also, since it is not necessary to phase match for an exact set of frequencies as in second-harmonic generation, the angular alignment and temperature of the crystal are far less critical.

From Eqs. (14) and (6) it is seen that a measurement of the ratio of spontaneously emitted power to incident power at a known temperature and signal wavelength yields the ratio of d_{15}^2/b . It is thus clear that if d_{15} is desired, the dispersion constant b must be determined. A number of alternatives are available. First, a relatively short crystal could be used and the aperture closed down until the minimum bandwidth is reached, where then $(\text{bandwidth})_{\min} = 0.885/bL$. Alternatively, it may be shown by examining Eq. (13) that, for $\theta^2 \gtrsim 2\pi/Lg$, the bandwidth is given by the following:

$$\text{bandwidth} = (g/2\pi b)\theta^2, \quad (16)$$

where g is given by Eq. (12). This latter technique allows the measurement of b at more easily measured bandwidths or by the measurement of the slope of the bandwidth-versus- θ^2 curve. A third alternative is to measure the refractive indices of the crystal by conventional techniques and thus determine b directly.

From the slope of Fig. 3, we obtain $P_s/P_p = 0.18 \times 10^{-4}\theta^2$, which from Eqs. (6) and (14) yields $d_{15}^2/b = 5.13 \times 10^{-36}$. From Fig. 5 and Eq. (16) we obtain $b = 6.2 \times 10^{-10}$ sec/m, thus yielding $d_{15} = 0.55 \times 10^{-22} \pm 10\%$ in mks units which is in good agreement with the published value $d_{15} = 0.56 \times 10^{-22}$.^{14,15}

ACKNOWLEDGMENT

The authors gratefully acknowledge many helpful discussions with M. K. Oshman.

Atomic Arrangement in Vitreous Selenium

ROY KAPLOW, T. A. ROWE,* AND B. L. AVERBACH

*Department of Metallurgy and Materials Science, Massachusetts Institute of Technology,
Cambridge, Massachusetts*

(Received 6 December 1967)

X-ray diffraction data at 25 and -196°C have been used to obtain radial distribution functions for amorphous and hexagonal selenium. The amorphous selenium exhibited strong correlation peaks at 2.34, 3.75, 5.8, 7.2, and 9.3 Å, with minor peaks at 4.3, 4.7, 5.1, 7.7, 10.0, and 10.5 Å. The first two distances are observed in both the hexagonal form, which consists of spiral chains, and the monoclinic forms, which consist of eight-membered puckered rings. The remaining major peaks do not correspond to intramolecular distances in any of the crystalline forms. Attempts were made to match the experimental amorphous distribution function with models which involved perturbations of the atom positions in the hexagonal and in the two monoclinic crystalline forms. A computer array consisting of 100 atom positions was used, and perturbations were chosen by a Monte Carlo procedure which allowed only those perturbations which improved the fit to the experimental distribution function. It was shown that relatively small rms static displacements, of the order of 0.20 Å, were sufficient to convert the monoclinic ring structures to the observed vitreous form, whereas much larger perturbations, of the order of 0.7 Å, were required to convert the hexagonal chain structure into a form which would give a suitable amorphous radial distribution function. The atomic configurations in the perturbed monoclinic structures consisted mainly of slightly distorted rings. There were a few locations where the rings had been opened sufficiently so that the atoms in the vicinity of the opening appeared to have the nearest-neighbor trigonal symmetry of the chain rather than of the eight-membered ring. The optical and Raman spectra provide strong evidence for the presence of Se_8 rings and a weaker indication of near-neighbor trigonal symmetry. We conclude that the structure of vitreous selenium consists mainly of slightly distorted Se_8 rings, along with an occasional ring which is opened sufficiently to develop a weak localized trigonal symmetry or a few greatly deformed chains.

I. INTRODUCTION

THE atomic arrangement in amorphous selenium is not well established, in spite of several recent attempts to determine the structure. The problem is inherently more difficult than an analogous crystal-structure determination since diffraction data can be transformed no farther than a radial distribution function (RDF). An atomic model must then be postulated, including assumptions of thermal displacement and molecular configuration, and the corresponding radial

distribution function calculated. The experimental RDF is frequently plagued by false detail, and conversely, the calculation of an RDF from an atomic model is not a trivial procedure when a crystal lattice is absent. There has thus been great uncertainty in the results for selenium, and it frequently appears that the methods of amorphous-structure determination are being developed along with the structure.

There are two basic atomic arrangements in crystalline selenium. The hexagonal form is stable at room temperature; the atoms in this structure are arranged in long parallel chains with the threefold spiral about the

* Present address: Fairchild Semiconductor, Palo Alto, Calif.